Biosensors and Bioelectronics 55 (2014) 417–422

Contents lists available at ScienceDirect

Biosensors and Bioelectronics

journal homepage: www.elsevier.com/locate/bios

Nano-yeast–scFv probes on screen-printed gold electrodes for detection of *Entamoeba histolytica* antigens in a biological matrix

Yadveer S. Grewal [a], Muhammad J.A. Shiddiky [a,*], Lauren J. Spadafora [c], Gerard A. Cangelosi [c], Matt Trau [a,b,*]

[a] Centre for Biomarker Research and Development, Australian Institute for Bioengineering and Nanotechnology (AIBN), The University of Queensland, Brisbane QLD 4072, Australia
[b] School of Chemistry and Molecular Biosciences, The University of Queensland, Brisbane QLD 4072, Australia
[c] School of Public Health University of Washington, Seattle, WA, USA

ARTICLE INFO

Article history:
Received 9 October 2013
Received in revised form
4 December 2013
Accepted 18 December 2013
Available online 27 December 2013

Keywords:
Nano-yeast–scFv
Affinity reagent
Electrochemical immunosensor
Screen-printed electrode
Entamoeba histolytica
Label-free detection

ABSTRACT

The time and costs associated with monoclonal antibody production limit the potential for portable diagnostic devices to penetrate the market. Replacing the antibody with a low-cost alternate affinity reagent would reduce the costs of diagnostic development and use, and lead to new portable diagnostic devices towards many diseases. Herein, we present low-cost affinity reagents, nano-yeast–scFv, on commercially available, inexpensive, and portable screen-printed electrodes for the label-free electrochemical detection of *Entamoeba histolytica* cyst antigens. The biosensor was able to detect antigen at concentrations down to 10 pg mL^{-1} in buffer with an inter-assay reproducibility of (% RSD, $n=3$) 4.1%. The applicability of two differently engineered nano-yeast–scFv to each specifically detect their cognant *E. histolytica* cyst antigens was demonstrated in a biological matrix derived from human stool. Because of the simple, inexpensive, and sensitive nature of this methodology, it may offer a low-cost alternative to immunosensors based on antibody-target recognition.

1. Introduction

Developing countries and remote areas require diagnostics that are portable, low-cost, quick, and easy to use, to ensure patients are expeditiously and accurately treated to control the spread of infectious disease (Mabey et al., 2004). In these regions, laboratory tests are often not viable for reasons of cost and logistics (Mabey et al., 2004). Screen-printed electrodes are inexpensive single-use electrodes (Metters et al., 2011), that are produced by printing various inks, such as gold and carbon, on different types of plastics or ceramics (Dominguez Renedo et al., 2007). Due to their relative low cost compared to traditional electrode materials, screen-printed electrodes can be suitable components in future point-of-care devices. Electrochemical biosensors utilizing screen-printing technology have found commercial success for diabetes management (Heller and Feldman, 2008), and have been demonstrated for the detection of various waterborne pathogens (Deng et al., 2013; Laczka et al., 2013; Yean et al., 2008).

Entamoeba histolytica (*E. histolytica*) is waterborne pathogen which causes up to 100 000 deaths annually in developing countries (Tanyuksel and Petri, 2003), and as such, it has been the focus of diagnostic development to accurately detect *E. histolytica* infection at point of care (Leo et al., 2006). Microscopy and serology are common diagnostic techniques, however, these are (respectively) inadequate in accurately identifying *E. histolytica* from closely related non-pathogenic commensals in stool and discriminating from past and current infection (Haque and Petri, 2006; Tanyuksel and Petri, 2003). Additionally, PCR tests towards *E. histolytica* are increasingly common (Paglia and Visca, 2004; Roy et al., 2005), but they are too expensive for most settings where *E. histolytica* disease is endemic. New specific and sensitive detection tests are required to overcome these limitations. Molecular tests, such as enzyme-linked immunosorbent assay (ELISA), are able to fulfill these criteria, and are now favored tests to identify *E. histolytica* infection (Haque and Petri, 2006).

ELISA-based methods are limited by their dependence on highly specific affinity reagents, typically monoclonal antibodies (mAbs). The generation of mAbs necessitates considerable costs in time and resources. This has constrained advancements in biomedical research and diagnostic development. Single-chain variable fragments (scFv) are affinity reagents which have the potential to overcome the limitations imposed by mAbs (Holliger and Hudson, 2005). Unlike

* Corresponding authors. Tel: +61 7 33464178; Fax: +61 7 33463973.
E-mail addresses: m.shiddiky@uq.edu.au (M.J.A. Shiddiky), m.trau@uq.edu.au (M. Trau).

0956-5663/$ - see front matter © 2013 Elsevier B.V. All rights reserved.
http://dx.doi.org/10.1016/j.bios.2013.12.043

traditional vertebrae animal-derived mAbs, scFv reagents can be inexpensively and quickly selected from a yeast- (or phage-) display library.

There are numerous demonstrations of biosensors incorporating scFv affinity reagents (Backmann et al., 2005; Shang et al., 2012; Shen et al., 2008; Torrance et al., 2006; Zeng et al., 2011); however, many scFvs derived from display libraries perform unsatisfactorily in solution (Miller et al., 2005). ScFv reagents culled from a display library are products of selection. Unfortunately, selected scFv fragments, which have excellent activity on yeast surfaces often lose their activity once in solution, an environment for which they were not selected. This decrease in activity has hindered adaption of scFv into diagnostic practice. To address this limitation, lyophilized whole yeast cells with displayed scFv (yeast–scFv) have been shown to function directly as affinity reagents and have been developed as low-cost, renewable alternatives to mAbs (Gray et al., 2012). Yeast–scFv can be quickly produced in vast quantities at a much lower cost than mAbs. However, yeast–scFvs are insoluble and too large for the adaption into many diagnostic applications. Yeast–scFv also require labeled secondary polyclonal antibodies to detect antigen binding to the yeast–scFv particles, hence complicating assay development and performance.

To address yeast–scFv limitations, we previously developed cell-free yeast–scFv affinity reagents by mechanical fragmentation of yeast–scFv cells. Cell wall fragments bearing displayed scFv were enriched by binding to surface-attached antibodies specific to the scFv′s epitope tags. These reagents, herein referred to as nano-yeast–scFv, have been developed as a replacement for monoclonal antibodies (Grewal et al., 2013). This concept demonstrated the detection of a single antibody/antigen capture combination in a defined buffer medium, using laboratory-dependent gold disc macroelectrodes.

Faradaic electrochemical impedance spectroscopy (F-EIS) is a highly effective method for the label-free detection of biomolecules (Katz and Willner, 2003; Zhou and Dong, 2011). Successful capture and detection of the biomolecule of interest using nano-yeast–scFv capture probe causes an observable change in the capacitance and interfacial electron transfer resistance of a conductive electrode (Katz and Willner, 2003; Zhou and Dong, 2011). A F-EIS spectrum on a screen-printed electrode is commonly presented in the form of a Nyquist plot with Z' *versus* Z'' at variable frequencies, and where Z' and Z'' are the real and imaginary components, respectively (Bard and Faulkner, 2000). At higher frequencies, the semicircle portion of the Nyquist plot is observed, which corresponds to the electron-transfer-limited process (Bard and Faulkner, 2000; Katz and Willner, 2003). The semicircle diameter is directly related to the electron-transfer resistance at the electrode surface, $\boldsymbol{R}_{ct}$. Consequently, stepwise construction of the immunosensing layer and capture of antigen by the nano-yeast–scFv complex can be observed by F-EIS, where the impedance change of the interface between the electrode surface and electrolyte solution, containing a redox probe (*e.g.*, $[Fe(CN)_6]^{3-/4-}$), is measured in the form of its $\boldsymbol{R}_{ct}$.

To develop and demonstrate nano-yeast–scFv as alternative affinity reagents in diagnostics, we have now combined these inexpensive affinity reagents with commercially available disposable screen-printed gold electrodes, in place of the more expensive gold disk electrodes used previously (Grewal et al., 2013). We then validated the system by using it to detect recombinant *E. histolytica* antigens spiked into a complex biological matrix derived from human stool. Furthermore, a second set of nano-yeast–scFv detecting an alternative *E.histolytica* antigen was examined with our system. This new combination indicates that like mAbs, nano-yeast–scFv can routinely be engineered to specifically capture any antigen of interest. The combination of nano-yeast–scFv screen-printed electrode platform with the ease of label-free electrochemical detection allows for simple, quick, and cheap analysis of *E. histolytica* antigens.

2. Materials and methods

2.1. Chemicals and materials

All chemicals purchased from the Australian supplier′s branch, unless otherwise stated. Stool samples, lyophilized yeast–scFv, and *E. histolytica* antigens EHI_115350, EHI_182030, and EHI_044550 (called '350', '030', and 'Jacob' respectively) in this report were produced by The University of Washington, USA and Seattle Structural Genomics Center for Infectious Disease (SSGCID). Biotinylated anti-HA antibody (Bio anti-HA) was purchased from Sapphire Bioscience. Biotinylated bovine serum albumin (BSA) was obtained Thermo scientific. Streptavidin was procured from Invitrogen. Phosphate buffered saline (PBS) tablets were purchased from Astral Scientific. Potassium ferrocyanide, potassium ferricyanide, and potassium chloride were all purchased from Sigma Aldrich. Protease Inhibitor EDTA-free cocktail tablets were obtained from Roche. Glycerol was procured from Ajax Finechem. Screen-printed gold electrodes, DRP-C220BT (geometric area = 0.126 cm^2), were acquired from Dropsens, Spain. Millex-VV 0.1 μm, Durapore PVDF (diameter 33 mm), low protein binding syringe filters were purchased from Millipore. The effective working area (=0.180 cm^2) of the screen-printed gold electrodes were determined under linear sweep voltammetric conditions for the one-electron reduction of $K_3[Fe(CN)_6]$ [1.0 mM in water (0.5 M KCl)] and use of the Randles-Sevcik relationship (Bard and Faulkner, 2000; Grewal et al., 2013).

Residues 135–271 of antigen EHI_115350 ('350') were expressed recombinantly in *E. coli* in a modified, N-terminal 6xHis pET11b vector and purified by Ni-NTA IMAC. Residues 159–481 of EHI_044550 ('Jacob') were expressed in a pE-SUMO vector (Life Sensors), also purified by Ni-NTA IMAC, and cleaved from the His-SUMO tag by SUMO protease digestion. Full-length EHI_182030 ('030') was expressed in *E. coli* and purified in Tier 1 of SSGCID(Bryan et al., 2011; Stacy et al., 2011).

The yeast–scFv library was a generous gift from K. Dane Wittrup. Antigens '350' and '030' were biotinylated with EZ-Link NHS-PEG4 biotin (Thermo Pierce), respectively. Yeast selections were conducted as before (Chao et al., 2006; Gray et al., 2012). In brief, two rounds of magnetic selection were conducted on the induced library with 100 nM of a biotinylated antigen and streptavidin (R1)- or α-biotin(R2)-conjugated beads (Milentyi). The resultant output was further enriched for bio-antigen/SA-PE and α-myc-FITC double-positive cells through two rounds on a Beckman Aria II cell sorter. After plating, individual clones were confirmed to be antigen specific by flow cytometry analysis, and clone diversity was determined by scFv PCR amplification and BstNI digest (New England Biosciences, USA).

The stool matrix was derived from human samples collected by the International Centre for Diarrheal Disease Research, Bangladesh (ICDDR,B) with institutional review board approval from the University of Washington and the ICDDR,B. Five 1–2 mL *Entamoeba histolytica*-negative samples were combined, diluted 1:1 in PBS, and spun at high speed for 5 min. The supernatant was collected and disinfected by boiling for 10 min at 90 °C. Before use, disinfection was confirmed by three days absence of microbial growth on tryptic soy and nutrient agar plates.

2.2. Generation of nano-yeast–scFv

After confirmation of specific antigen binding, the cells were lyophilized for long-term storage as described (Gray et al., 2012), following a modified protocol that added 10% dextran and 5%

sodium glutamate to yeast. Nano-yeast–scFv were created as previously described (Grewal et al., 2013), with a modified protocol that added sodium azide. Briefly, lyophilized yeast was disrupted with a mortar and pestle into a fine powder, then 10 mL of PBS, 5% glycerol and protease inhibitor cocktail were added. The sample was centrifuged at 500 RCF for 2 min at 15 °C to remove whole yeast. To prevent microbial growth, sodium azide 0.05% was added. The processed lysates (supernatant) were stored at 4 °C until use and filtered using a 0.1 μm filter.

2.3. Assay protocol

Screen-printed gold electrodes were functionalized with BSA by incubating them in 700 μl of biotinylated BSA solution (500 $\mu g mL^{-1}$) for 1 h at 25 °C on an intelli-mixer (PCOD Scientific) with gentle agitation. These intelli-mixer settings were used in all subsequent steps. The electrodes were then stored overnight at 4 °C. The electrodes were then washed with 1XPBS (pH 7.4, 137 mM sodium chloride, 2 mM potassium chloride, 10 mM phosphate buffer) after each incubation step. The electrode was incubated in 700 μL of streptavidin (500 $\mu g\ mL^{-1}$). These functionalized electrodes were then treated with 100 $\mu g\ mL^{-1}$ of biotinylated HA antibody solution at room temperature for another hour, leading to immobilization of the anti-HA antibody on the electrode surface. Finally the nano-yeast–scFv reagent diluted 1/5 in PBS was allowed to bind (by virtue of the interaction between anti-HA and the HA affinity tag cloned into the yeast-display scFv) for 1 h before washing with PBS. This step tethered the nano-yeast–scFv to the electrode surface while at same time removing yeast fragments that do not bear displayed scFv. The electrodes were then incubated in 700 μL of antigen solution (spiked in either PBS or stool) at varying concentrations to complete the immunoreactions.

2.4. Electrochemical procedure

All electrochemical experiments were conducted at room temperature (25 ± 1 °C) using screen-printed gold electrodes which comprised of an Ag reference, gold counter, and a 4 mm diameter gold working electrode using an electrochemical analyzer CHI 650D (CH Instruments, Austin, TX). Electrochemical measurements were measured in a 10 mM phosphate buffer solution (pH 7.4) containing 2.5 mM $[Fe(CN)_6]^{3-}/[Fe(CN)_6]^{4-}$ (1:1) and 0.1 M KCl. Differential pulse voltammetric (DPV) signals were obtained with a potential step of 5 mV, pulse amplitude of 50 mV, pulse width 50 ms, and a pulse period of 100 ms. The EIS spectra were recorded using an alternating current voltage of 10 mV, with the frequency range of 1 Hz–100 kHz.

3. Results and discussions

Fig. 1 outlines our approach for the label-free detection of *E. histolytica* antigens using nano-yeast–scFv affinity reagents on screen-printed electrodes. Briefly, the gold electrode is coated with a biolayer of biotinylated BSA (1. Bio-BSA). Streptavidin (2. Streptavidin) is then used to link the bio-BSA to a biotinylated anti-human influenza hemagglutinin tag antibody (3. Bio anti-HA). Nano-yeast–scFv (prepared from yeast–scFv clone '350-E2' or '030-L') is then captured by the use of a HA antigen tag cloned into the recombinant scFv construct (4. Nano-yeast–scFv). The bound nano-yeast–scFv is then used to capture the target *E. histolytica* antigens ('350' or '030') (5. *E histolytica* antigen). The utilized yeast-display library was constructed with the scFv already fused to HA and c-myc tags (Feldhaus et al., 2003). Thus, beyond the 2–4 weeks required to isolate the yeast–scFvs, only a single, commercially available ("off-the-shelf") biotinylated anti-

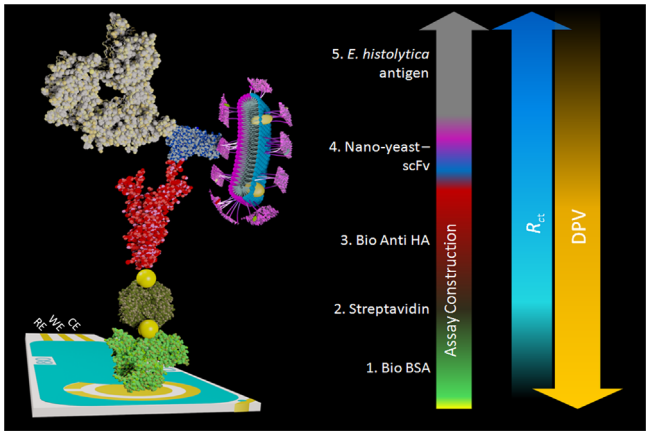

Fig. 1. Schematic of label-free protein detection on gold coated screen-printed electrode. *E. histolytica* proteins complexed with screen-printed gold working electrode (WE) surface attached with nano-yeast–scFv fragments which results in an increase of $\boldsymbol{R}_{ct}$ and, inversely, a decrease of DPV.

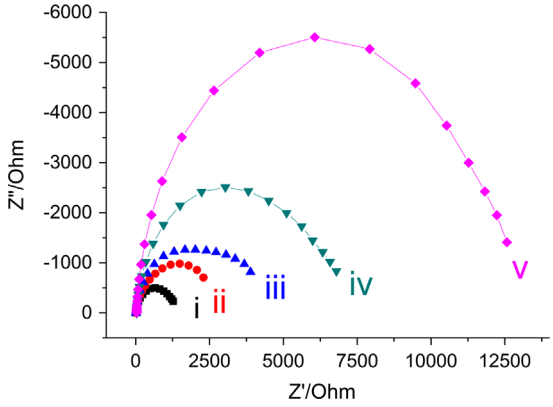

Fig. 2. Nyquist plot for (i) bio-BSA, (ii) bio-BSA/streptavidin, (iii) bio-BSA/streptavidin/bio anti-HA, (iv) bio-BSA/streptavidin/bio anti-HA/ nano-yeast–scFv and (v) bio BSA/streptavidin/bio anti-HA/ nano-yeast–scFv/ '350' immunocomplex in 10 mM phosphate buffer solution (pH 7.4) containing 2.5 mM $K_3[Fe(CN)_6]$, 2.5 mM $K_2[Fe(CN)_6]$, and 0.1 M KCl.

HA mAb was required to build the assay. This approach is far more cost effective than making monoclonal antibodies for every different antigen.

The attachment of the bio-BSA, streptavidin, bio anti-HA, nano-yeast–scFv and *E. histolytica* antigens on the gold coated screen-printed electrode was measured by F-EIS (Fig. 2). The assay complex blocks the interfacial electron transfer reaction of $[Fe(CN)_6]^{3-/4-}$, subsequently increasing the $\boldsymbol{R}_{ct}$. We observed an increase in $\boldsymbol{R}_{ct}$ from the successive blocking of the electrode surface with the stepwise attachment of the streptavidin, the bio ant-HA, and the nano-yeast–scFv onto the bio-BSA modified screen-printed electrode (Fig. 2). There was a clear increase of the $\boldsymbol{R}_{ct}$ generated from the $[Fe(CN)_6]^{3-/4-}$ process in the presence of *E. histolytica* antigen (Fig. 2 (v)). The bio BSA modified screen-printed electrode (Fig. 2 (i)) gave rise to the lowest semicircle domain, followed by bio BSA modified/streptavidin (Fig. 2 (ii)), bio anti-HA (Fig. 2 (iii)), nano-yeast–scFv (Fig. 2 (iv)), and target antigen (500 $pgmL^{-1}$) (Fig. 2 (v)). These results indicate successful stepwise construction of the biosensor. The biosensor showed good reproducibility with less than 5% relative standard deviation (RSD) between the inter-assay signals, at each step of the assay: (i) 1.2%, (ii) 2.13%, (iii) 4.76%, (iv) 3.00%, (v) 4.01%, $n=3$. To validate the assay construction as well as to assess the risk of possible false positive impedimetric responses in our assay, a series of control DPV measurements were conducted (data not shown) using

biomolecule functionalized electrodes. The peak current decreases in response to an increase in the hindrance (*i.e.*, via successive biomolecules attachment) of the electron transfer reaction of $[Fe(CN)_6]^{3-/4-}$ process.

The specificity of the immunosensor towards '350' antigen on the gold coated screen-printed electrode was examined by attempting to capture an antigen that was non-specific to the nano-yeast–scFv probe. The 'Jacob' protein was previously shown not to bind with the '350-E2' yeast–scFv clone (Gray et al., 2012; Grewal et al., 2013) or with '350-E2'-derived nano-yeast–scFv (Grewal et al., 2013). Non-specific binding of the 'Jacob' protein was evaluated by using F-EIS measurements. A high concentration of the 'Jacob' protein (1 ng mL^{-1}) was used to determine the detection of background binding (Fig. 3 (ii)). The signals observed for with 'no antigen' case were essentially identical with the 'Jacob' (Fig. 3 (ii) and (iii)). This indicates that the assay system detects the bulky anti-HA-nano-yeast–scFv complex, but without significant cross-reaction with 'Jacob'. Comparatively, the $\boldsymbol{R}_{ct}$ increase produced by the target '350' antigen at 500 pg mL^{-1} (Fig. 3 (iv)) was much greater. This indicates that nano-yeast–scFv retain their specificity (Grewal et al., 2013) towards target antigen. To assess background noise an assay was performed which excluded the nano-yeast–scFv layer (Fig. 3 (i)). Non-specific absorption and interaction of the '350' antigen on the bio-BSA/streptavidin/bio anti-HA screen-printed electrode was examined (Fig. 2 (iii) *vs.* Fig. 3 (i)), however the $\boldsymbol{R}_{ct}$ signal increase was small, which indicates that non-specific absorption was minimal.

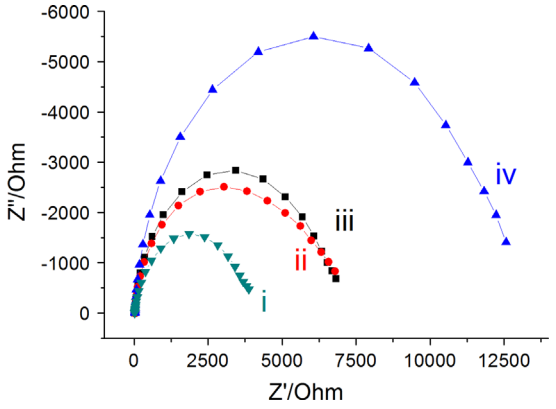

Fig. 3. Nyquist plot for (i) bio-BSA/streptavidin/bio anti-HA/'350' at 500 pg mL^{-1} (no nano-yeast–scFv reagent), (ii) bio-BSA/streptavidin/bio anti-HA/nano-yeast–scFv (no antigen), (iii) bio-BSA/streptavidin/bio anti-HA/nano-yeast–scFv/ 'Jacob' at 1000 pg mL^{-1}, and (iv) bio-BSA/streptavidin/bio anti-HA/ nano-yeast–scFv/ '350' at 500 pg mL^{-1} complex formation in 10 mM phosphate buffer solution (pH 7.4) containing 2.5 mM $K_3[Fe(CN)_6]$, 2.5 mM $K_2[Fe(CN)_6]$, and 0.1 M KCl.

The reproducibility of F-EIS measurements for '350' antigen was determined to be a RSD of 4.51% ($n=3$), while 'Jacob' measurements was found to have a RSD of 3.88% ($n=3$) and 'no antigen' case was determined to have a RSD of 3.00% ($n=3$).

The dynamic range of detection for antigen '350' using nano-yeast–scFv on screen-printed electrode was measured before and after the nano-yeast–scFv modified electrode was incubated with designated concentrations of '350' antigens (1 pg mL^{-1} to 1 ng mL^{-1}). The $\boldsymbol{R}_{ct}$ signal increased with increasing amounts of antigen concentration (Fig. 4 (A) and (B)). The presence of antigen detected is accounted by faradic current generated by $K_3[Fe(CN)_6]^{3-}/[Fe(CN)_6]^{4-}$ probe. The relative $\boldsymbol{R}_{ct}$ changes corresponding to antigen binding to the nano-yeast–scFv (Fig. 4 (B)) was calculated as follows:

$$\%\ \text{change of}\ R_{ct} = \Delta R_{ct} = (R_{ct,after} - R_{ct,before})/R_{ct,before} \times 100 \quad (1)$$

where $\boldsymbol{R}_{ct,\ before}$ was the mean $\boldsymbol{R}_{ct}$ at zero concentration ($\boldsymbol{R}_{ct}$ for bio-BSA/streptavidin/bio anti-HA) and $\boldsymbol{R}_{ct,\ after}$ was the mean $\boldsymbol{R}_{ct}$ at any concentration of the '350' antigen.

The lower limit of detection was confirmed down to 10 pg mL^{-1} (588 fM). This concentration of antigen detected is ten times more sensitive than our previously reported limit of detection for '350' antigen on a gold disk electrode (Grewal et al., 2013) and about 550 times more sensitive than detecting *E. histolytica* antigen using whole-cell yeast–scFv with fluorescently labeled signal antibodies (Gray et al., 2012). This lower limit of detection is also comparable to the detection of antigen using ELISA and a typical IgG mAb. This increased sensitivity may be attributed in part to the presence of gold particles on the screen-printed electrode surface (the commercially obtained screen printed electrodes uses a gold ink that is cured at 120 °C, which forms a rough working surface of gold particles). Gold particles are known for their high electrocatalytic activity allowing for increased sensitivity of biomolecule detection using impedance and other electrochemical measurements (Cederquist and Kelley, 2012; Li et al., 2005). The linear dynamic range of the assay was determined to be from 10 pg mL^{-1} (588 fM) to 500 pg mL^{-1} (29.4 pM). Reproducibility of the concentrations was examined on three separate electrodes, resulting in a RSD of $<4.1\%$ between the electrodes at each concentration.

E. histolytica cysts are detected in patient stool samples for diagnosis of *E. histolytica* infection. Therefore, the ability to detect cyst antigens in stool matrix is a crucial requirement when designing a clinical diagnostic. Antigens '350' and '030' (each 500 pg mL^{-1}) were spiked into a biological matrix comprised of disinfected (for occupational safety) stool diluted 1/5 in PBS. The $\boldsymbol{R}_{ct}$ signal of the assay complex containing the '030-L' nano-yeast–scFv sensing layer in stool (Fig. 5 (B (i)), showed a slight increase

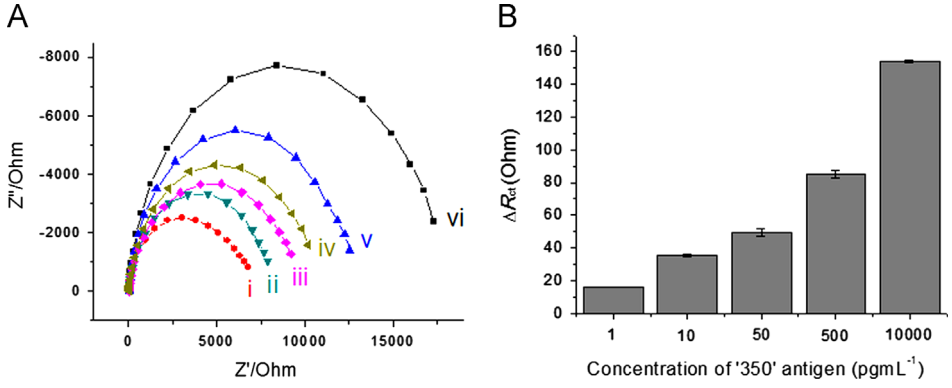

Fig. 4. (A) Nyquist plot of the F-EIS responses at the immunosensing surface after incubation with designated concentrations of *E. histolytica* '350' antigen at (i) 0 (ii) 1 pg mL^{-1} (iii) 10 pg mL^{-1} (iv) 50 pgmL^{-1} (v) 500 pg mL^{-1} (vi) 1000 pg mL^{-1}. (B) Relative change of the $\boldsymbol{R}_{ct}$ responses, normalized to the 'zero-antigen' signal, at the immunosensing surface after incubation with designated concentrations of *E. histolytica* '350' antigen. Each data point represents the average of three separate trials ($n=3$) and error bars represent standard error of measurements within each experiment.

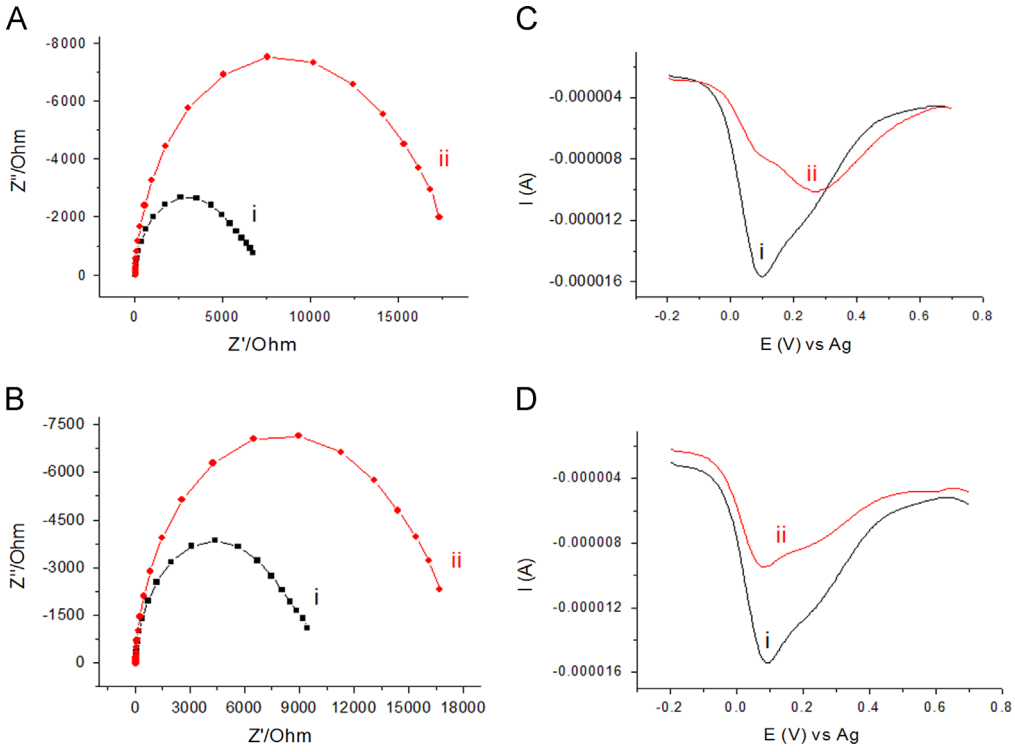

Fig. 5. Nyquist plot for (A) (i) assay with no antigen, (ii) cognate '350,' and (B) (i) assay with no antigen, (ii) cognate '030' antigen in stool with 10 mM phosphate buffer solution (pH 7.4) containing 2.5 mM $K_3[Fe(CN)_6]$, 2.5 mM $K_2[Fe(CN)_6]$, and 0.1 M KCl. Antigens '350' and '030' concentrations were 500 pgmL^{-1}. Stool diluted 1/5 in PBS. Corresponding DPV responses for antigen (C) '350' and (D) '030'.

compared to the '350-E2' nano-yeast–scFv complex in PBS (Fig. 3 (ii)) and stool (Fig. 5 (A (i)). This signal increase may be attributed to low levels of non-specific adsorption of stool biomolecules on the immunosensor. For both antigens, a clear increase in signal was observed when antigen was spiked into the sample compared to the 'no antigen control' (Fig. 5 (A) and (B)). The F-EIS measurements were found to have a RSD of 9.88% and 8.45% ($n=3$) for inter-assay signals for antigens '350' and '030', respectively. Fig. 5 (C) and (D) shows the differential pulse profiles, where the current decreases due to increase hindrance of $[Fe(CN)_6]^{3-/4-}$ process. DPV peak current decreased when antigen was captured, compared to the assay complex without antigen (Fig. 5 (C) and (D)). This is in line with the F-EIS responses (Fig. 5 (A) and (B)). This indicates that our current diagnostic platform has sufficient specificity to successfully detect *E. histolytica* antigens in a complex biological matrix. Thus our biosensor has demonstrated the potential of nano-yeast–scFv affinity reagents to detect antigens in clinical samples. A commercial ELISA kit is currently available for *E. histolytica* detection in stool (TechLab *E. histolytica* II test). This diagnostic detects the trophozoite protein Gal/GalNAc lectin, which is different from our target cyst antigens. The commercial TechLab kit uses highly optimized antibodies and has been reported to detect its target antigen at concentrations of ~1000 pg mL^{-1} in stool (Fotedar et al., 2007). Thus, the analytical sensitivity of our system compares favorably to a commercial ELISA functioning in a similar biological matrix.

4. Conclusions

In conclusion, we have demonstrated nano-yeast–scFv affinity reagents on a low-cost commercial gold screen-printed electrode for the sensitive detection of *E. histolytica* antigens spiked into stool samples. This work is the first demonstration of nano-yeast–scFv on a portable low-cost platform and the first demonstration of using nano-yeast–scFv affinity reagents to detect antigens in a complex biological matrix. A new antibody/antigen recognition combination was also demonstrated, consistent with the expectation that new nano-yeast–scFv affinity reagents can be routinely engineered towards diverse target antigens. Coupling a commercially available battery operated portable potentiostat with our nano-yeast–scFv coated screen-printed gold electrode would allow for field testing of *E. histolytica* antigens and potentially of other antigens that are of clinical interest. Because of this innovation, we envisage that nano-yeast–scFv has the potential to replace mAbs in point of care diagnostics.

Acknowledgments

This work was supported by the NIH Grant, USA (U01AIO82186-01) and ARC DECRA (DE120102503 to MJAS). Although not directly funding the research work in this paper, we acknowledge funding received by Trau's Laboratory from the National Breast Cancer Foundation of Australia *via* two National Collaborative Research Grants (CG-08-07 and CG-12-07). These grants have significantly contributed to the environment to stimulate the research described here. We would like to thank Annie L. Becker for coordinating with the institutional review board for the ethics approval for the stool samples, the Seattle Biomed Flow Cytometry Core for the cell sorting, and Maria Kahn at PATH for lyophilizing yeast–scFv for some experiments.

References

Backmann, N., Zahnd, C., Huber, F., Bietsch, A., Plückthun, A., Lang, H.-P., Güntherodt, H.-J., Hegner, M., Gerber, C., 2005. Proc. Natl. Acad. Sci. USA 102, 14587–14592.

Bard, A.J., Faulkner, L.R., 2000. Electrochemical Methods: Fundamentals and Applications. John Wiley & Sons.

Bryan, C.M., Bhandari, J., Napuli, A.J., Leibly, D.J., Choi, R., Kelley, A., Van Voorhis, W.C., Edwards, T.E., Stewart, L.J., 2011. Acta Crystallogr. Sect. F Struct. Biol. Cryst. Commun. 67, 1010–1014.
Cederquist, K.B., Kelley, S.O., 2012. Curr. Opin. Chem. Biol. 16, 415–421.
Chao, G., Lau, W.L., Hackel, B.J., Sazinsky, S.L., Lippow, S.M., Wittrup, K.D., 2006. Nat. Protoc. 1, 755–768.
Deng, W., Xu, B., Hu, H., Li, J., Hu, W., Song, S., Feng, Z., Fan, C., 2013. Sci. Rep., 3, http://dx.doi.org/10.1038/srep01789 (Article no. 1789).
Dominguez Renedo, O., Alonso-Lomillo, M.A., Arcos Martinez, M.J., 2007. Talanta 73, 202–219.
Feldhaus, M.J., Siegel, R.W., Opresko, L.K., Coleman, J.R., Feldhaus, J.M.W., Yeung, Y.A., Cochran, J.R., Heinzelman, P., Colby, D., Swers, J., Graff, C., Wiley, H.S., Wittrup, K.D., 2003. Nat. Biotechnol. 21, 163–170.
Fotedar, R., Stark, D., Beebe, N., Marriott, D., Ellis, J., Harkness, J., 2007. Clin. Microbiol. Rev. 20, 511–532.
Gray, S.A., Weigel, K.M., Ali, I.K.M., Lakey, A.A., Capalungan, J., Domingo, G.J., Cangelosi, G.A., 2012. PLoS ONE 7, e32042.
Grewal, Y.S., Shiddiky, M.J.A., Gray, S.A., Weigel, K.M., Cangelosi, G.A., Trau, M., 2013. Chem. Commun. 49, 1551–1553.
Haque, R., Petri Jr., W.A., 2006. Arch. Med. Res. 37, 272–275.
Heller, A., Feldman, B., 2008. Chem. Rev. 108, 2482–2505.
Holliger, P., Hudson, P.J., 2005. Nat. Biotechnol. 23, 1126–1136.
Katz, E., Willner, I., 2003. Electroanalysis, 15; , pp. 913–947.
Laczka, O., Skillman, L., Ditcham, W.G., Hamdorf, B., Wong, D.K.Y., Bergquist, P., Sunna, A., 2013. J. Microbiol. Methods 95, 182–185.
Leo, M., Haque, R., Kabir, M., Roy, S., Lahlou, R.M., Mondal, D., Tannich, E., Petri, W.A., 2006. J. Clin. Microbiol. 44, 4569–4571.
Li, C.-Z., Liu, Y., Luong, J.H.T., 2005. Anal. Chem. 77, 478–485.
Mabey, D., Peeling, R.W., Ustianowski, A., Perkins, M.D., 2004. Nat. Rev. Microbiol. 2, 231–240.
Metters, J.P., Kadara, R.O., Banks, C.E., 2011. Analyst 136, 1067–1076.
Miller, K.D., Weaver-Feldhaus, J., Gray, S.A., Siegel, R.W., Feldhaus, M.J., 2005. Protein Exp. Purif. 42, 255–267.
Paglia, M.G., Visca, P., 2004. Acta Trop 92, 273–277.
Roy, S., Kabir, M., Mondal, D., Ali, I.K.M., Petri, W.A., Haque, R., 2005. J. Clin. Microbiol. 43, 2168–2172.
Shang, Y., Mernaugh, R., Zeng, X., 2012. Anal. Chem 84, 8164–8170.
Shen, Z., Yan, H., Zhang, Y., Mernaugh, R.L., Zeng, X., 2008. Anal. Chem. 80, 1910–1917.
Stacy, R., Begley, D.W., Phan, I., Staker, B.L., Van Voorhis, W.C., Varani, G., Buchko, G.W., Stewart, L.J., Myler, P.J., 2011. Acta Crystallograph. Sect. F Struct. Biol. Cryst. Commun. 67, 979–984.
Tanyuksel, M., Petri, W.A., 2003. Laboratory diagnosis of Amebiasis. Clin. Microbiol. Rev. 16, 713–729.
Torrance, L., Ziegler, A., Pittman, H., Paterson, M., Toth, R., Eggleston, I., 2006. J. Virol. Methods 134, 164–170.
Yean, Kamarudin, Ozkan, B., Yin, D.A., Lalitha, L.S., Ismail, P., Ozsoz, A., Ravichandran, M., 2008. Anal. Chem. 80, 2774–2779.
Zeng, X., Shen, Z., Mernaugh, R., 2011. Anal. Bioanal. Chem. 402, 3027–3038.
Zhou, M., Dong, S., 2011. Acc. Chem. Res. 44, 1232–1243.